Oleksii Hyka[1], Andres Vejar[1,2], Tomasz Rymarczyk[1,2]

Netrix R&D Center (1), Wyższa Szkoła Ekonomii i Innowacji w Lublinie (2)
ORCID: 1.0000-0003-2129-5138; 2.0000-0002-2041-0387; 3.0000-0002-3524-9151

Data analysis system for surface potential of biological tissues

Abstract. A portable low-power monitoring system for measuring surface biopotential and data processing is presented. The small device was designed using hardware and codesign. The system is based on a microcircuit consisting of a field-programmable gate array device and a dual-core microcontroller. The selected reconfigurable hardware provides the desired level of speed and accuracy combined with low power consumption for online data processing applications. Spectroscopy impedance measurements are used to analyze the electrical properties of biological tissue.

*Streszczenie. Przedstawiono przenośny system monitorowania o niskim poborze mocy do pomiaru biopotencjału powierzchniowego i przetwarzania danych. Małe urządzenie zostało zaprojektowane z wykorzystaniem projektowania sprzętowego i kodowego. System oparty jest na mikroukładzie składającym się z programowalnej matrycy bramek oraz dwurdzeniowego mikrokontrolera. Wybrany rekonfigurowalny sprzęt zapewnia pożądany poziom szybkości i dokładności w połączeniu z niskim zużyciem energii dla aplikacji przetwarzania danych online. Pomiary impedancji w spektroskopii są wykorzystywane do analizy właściwości elektrycznych tkanki biologicznej (**Projektowanie systemu do analizy danych potencjału powierzchniowego na tkankach biologicznych**).*

Keywords: EIS, FPGA, biological tissues, FIR.
Słowa kluczowe: EIS, FPGA, tkanki biologiczne, FIR.

Introduction

The composition of the material can be indirectly observed by measuring the object's response with respect to excitation on its surface. For biological tissues, this method of measurement has recently expanded with the advent of smart devices for calculating body composition, for example, to estimate the percentage of fat, water, muscle, and bone in the body. The measurement method is based on electrical impedance spectroscopy (EIS). A modulated excitation signal is generated at different frequencies, and the response of the electrical potential of the object being tested is measured for each excitation frequency. Knowing the characteristics of each tomographic technique solution, the application allows the selection of a suitable image reconstruction method [1-6]. Different methods can be used to solve the optimisation process [7-8].

EIS can provide information about electrochemical reactions and the electrical properties of materials at the interface. Measuring an object at different frequencies allows you to monitor its impedance spectrum and compare the impedance spectrum of different objects. We can consider the impedance spectrum of an object as a signature. The material structure of two objects with the same signature can be the same. The applications for measuring surface potential and impedance changes are diverse and unique. Two critical applications of medicine are impedance plethysmography [9] and impedance cardiography [10]. Plethysmography impedance measures the impedance change at the skin's surface, which has been specifically designed to monitor volumetric changes. Impedance cardiography measures changes in impedance related to heart function. The special impedance measuring equipment is required considering the specific application. Accurate and consistent data for the measurement operation ensure correct evaluation with the appropriate level of quality. The key to ensuring reliable and accurate estimation is the compatibility of the measurement equipment and the implementation of algorithms in the software. Modern system devices (SoC) equipped with reconfigurable units (FPGA) and processing cores allow for a unified approach to system coding in specific measurement and analysis systems of hardware and software [3]. In this work, we use an SoC with two ARM processors and one FPGA [4] to create a complete device for measuring the electrical potential on the surface of biological tissues.

Proposed Measurement System and Hardware Architecture

The system we offer is based on the Xilinx Zynq-7000 SoC. The Zynq-7000 series provides a combination of ARM processors with standard microcontroller peripherals. The system is designed to provide high performance with low power consumption and portability.

The system has installed a Linux operating system for user-level programming, which facilitates data transfer over wireless computer networks (WAN). Figure 1 shows an overview of the system. The Zynq SoC consists of a programmable logic cell (Zynq PL) hardware and software processing system parts (Zynq PS). The digital signal generation and processing, and data acquisition are developed in FPGA hardware.
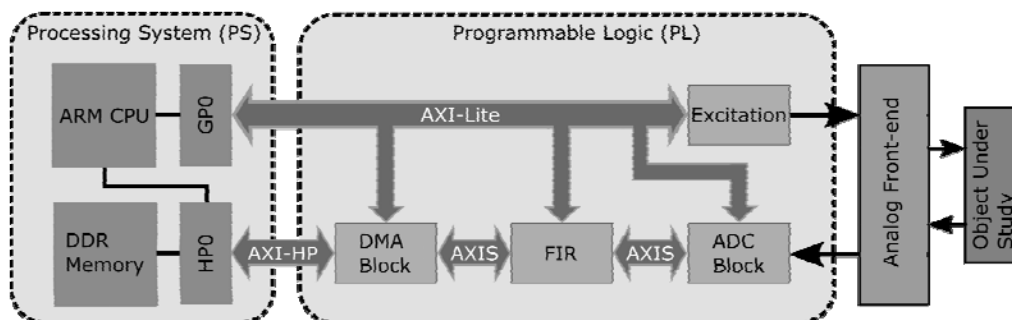
Fig.1. General overview of the system.

The system is used Intellectual Property (IP) on Vivado software to separate code between modules. IP modules have an input and output port for receiving and transmitting data and can be managed via AXI-Lite bus in shared memory between FPGA (Zynq PL) and the operating system (Zynq PS).

A Xilinx analogue-to-digital converter (XADC) was used to collect the excitation and sensing. XADC has a resolution of 12 bits, with a sampling rate of 1 MSPS [13]. The effective speed in our design is 0.86 MSPS per channel. The last application used two channels in serial mode. The Direct Memory Access (DMA) device was used to transmit data streams from PS to PL via a high-speed bus.

Figure 2 shows the block diagram of PS and PL. In the PS section, when the Zynq SoC starts, the system reads the default frequency value from the registry and updates the frequency value if it changes. At the same time, excitation, IP read frequency and start generating signal [14]. In addition, the Xilinx analogue-to-digital converter (XADC) starts reading data from the component under test. The ADC continuously converts the signal on both channels by switching the internal multiplexer (MUX) to serial mode.
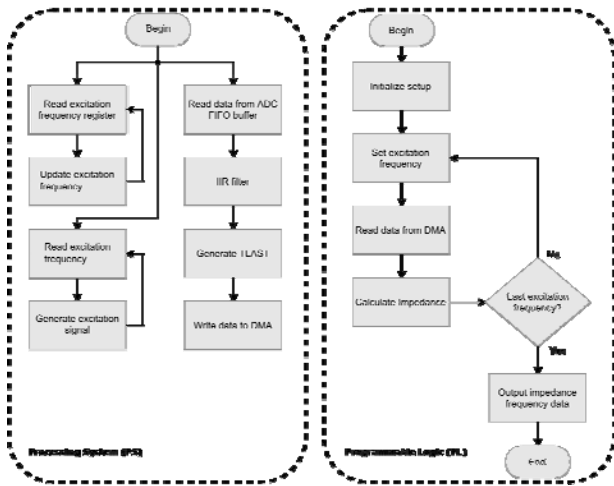
Fig. 2. Diagram of the data acquisition process considering PL and PS.

Data filtering was performed by adding a finite impulse response (FIR) filter. Data filtering was performed by adding a finite impulse response (FIR) filter. To write data from filter to DMA, data need to be prepared by creating packets with TLAST signal to perform data transmitting to DMA. TLAST is generating on our IP with the possibility to change a number of transmitted data by changing the register.

The script changes the excitation frequency and collects data from the DMA FIFO buffer. The data packet is parsed on two channels, and the impedance is calculated. The system continues the cycle until the expected frequency range is measured. The plots are presented at the end. The data is collected and stored on a local computer for further processing and presentation.

The proposed system can measure impedance from 300 Ω to 1 MΩ by manually changing the reference resistor. The system emits a square wave excitation signal from 3.6 V to peak. Our design controls the excitation potential to limit the current flowing through the test object. The current is usually 30 µA or less, depending on the high resistance of the test object.

Online filter on FPGA

For filtering data on real-time was used FIR compiler was provided by Xilinx. Measurement potential data are filtered after parsing ADC channels to split and send to independent FIR compilers.
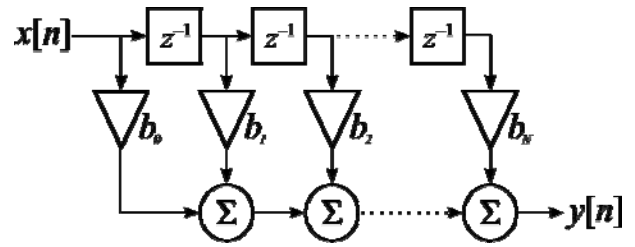
Fig. 3. Conventional Tapped Delay Line FIR Filter Representation.

Figure 3 shows the conventional tapped delay line realization of this inner-product calculation, and although the illustration is a useful conceptualization of the computation performed by the core, the actual FPGA realization is quite different.

The FIR compiler automatically selects the best algorithm of FIR implementation, depending on the design.
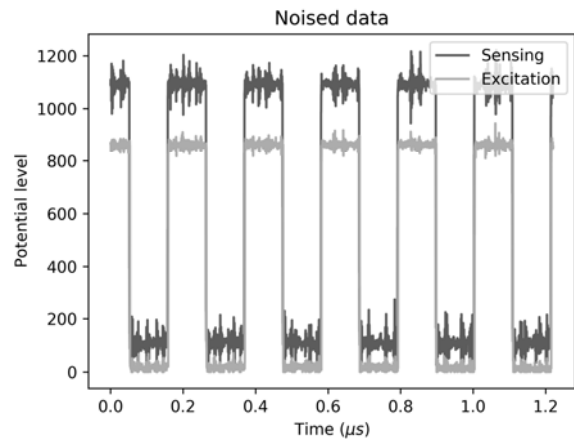
Fig. 4. Measured noised potential.
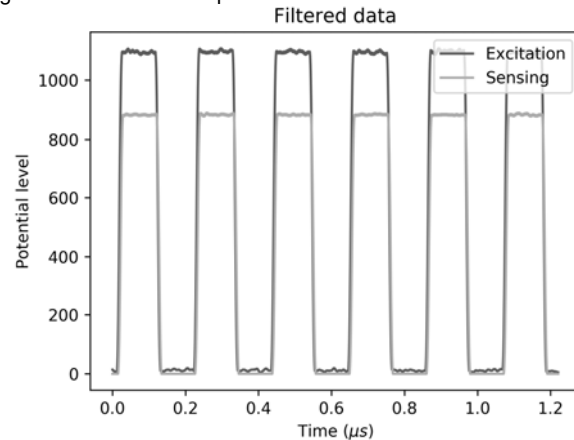
Fig. 5. Measured noised potential after FIR filter.

The FIR is configured to use fixed 57 coefficients in two-channel data filtering. Xilinx FIR IP has extra 8 bits of resolution after filtering due to averaging.

Figure 4 presents potential measurements of the system. The excitation frequency of the system is 2 kHz. In the plot, the ground was connected to add noise to the system to reproduce noise in biological measurements.

In Figure 5 are presented data passed through the FIR filter. As we can see, the filter is working well on filtering one of the difficult signals.

The impulse response of the FIR filter is presented in Figure 6. The impulse response in the firs subplot shows how every coefficient effect potential data. As we can see, the middle coefficients are most important and affect the data.
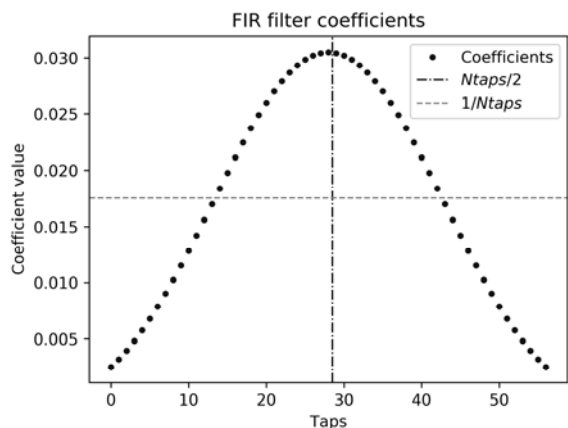
Fig.. 6. Significant of FIR coefficients.
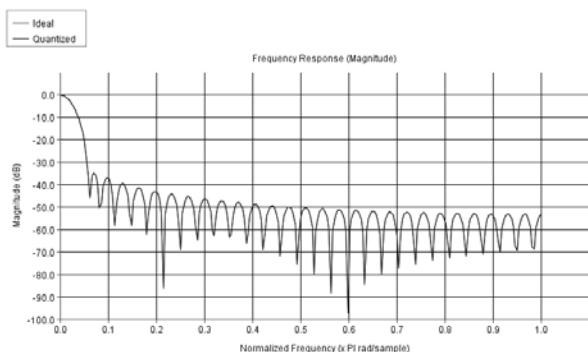
Fig.. 7. Frequency response of FIR filter.
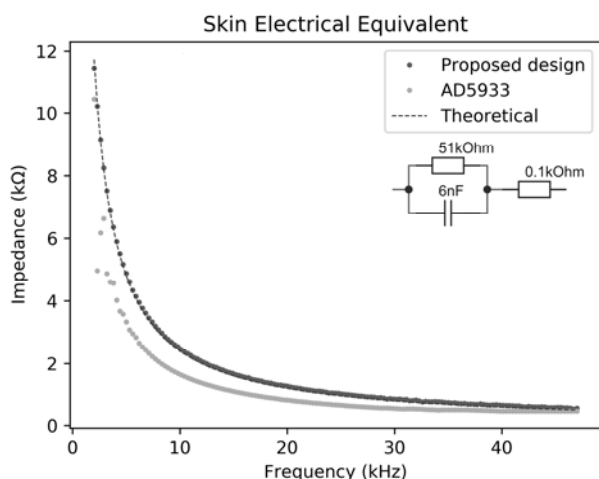
Fig.. 8. Impedance measurement of skin electrical equivalent circuit.
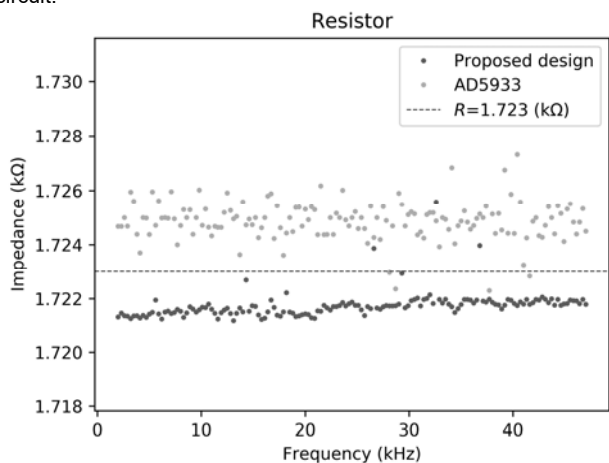
Fig. 9. Impedance measurement of constant phase element (resistor).

In Figure 7 are presented frequency response of the Low Pass FIR filter. The filter has a cut-off frequency of 16 kHz to keep the smallest number of coefficients. Therefore, the transition bandwidth is equal to 48 kHz.

Measurements and Validation

For validation of measurement, was selected EIS based on Eval AD5933 board.

In Figure 8 are presented results obtained from AD5933 and our system on measuring skin electrical equivalent circuit of. The SEES was created by connecting resistor and capacitor in parallel and resistor in serial. Our system is perfectly measuring this kind of circuit.

Measurement of constant phase element (resistor) is presented in Figure 9. The measurement was made in both of system and result of our design without averaging more stable than in AD5933.

Before measurement of biological tissues was decided to test our design on measuring subsurface impedance spectroscopy. EIS of fruits is presented in Figures 10-11. The measurements were made without averaging to show the stability of the system. As we can see, the impedance of fruits between boards is similar, but the shape of impedance reducing is different due to the integrated capacity on the board.
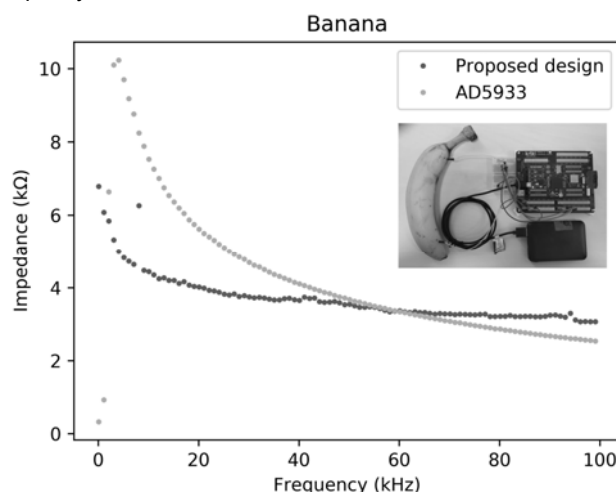
Fig. 10. Subsurface impedance measurement of apple.
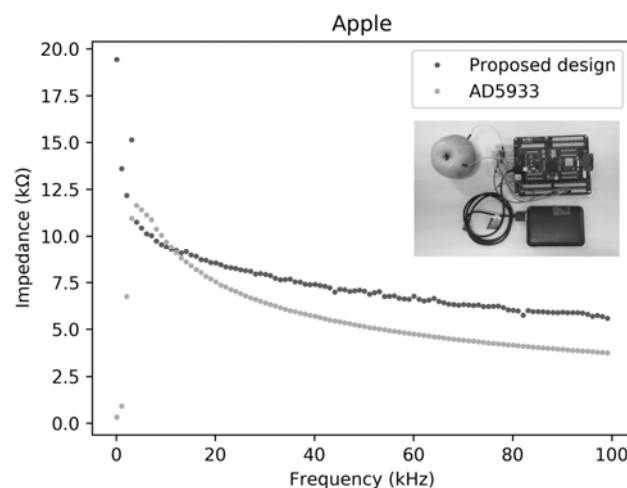
Fig. 11. Subsurface impedance measurement of banana.

Biological tissues measurement

For measuring biopotential, wet electrodes with gel [15] Figure 12 on wet skin to decrease the resistance of the first layer of skin.
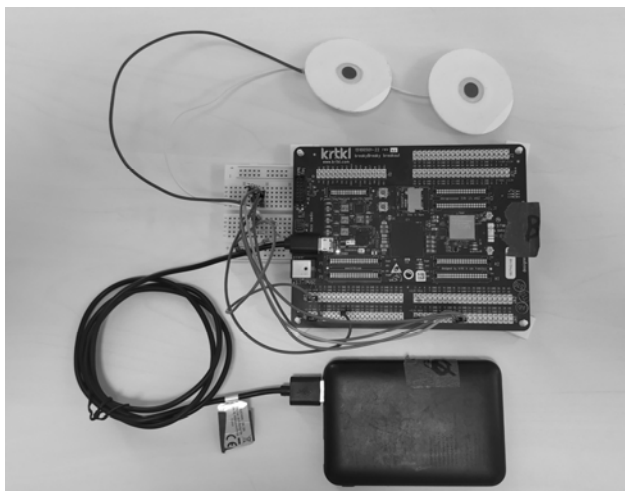
Fig..12. Setup for biopotential measurements.
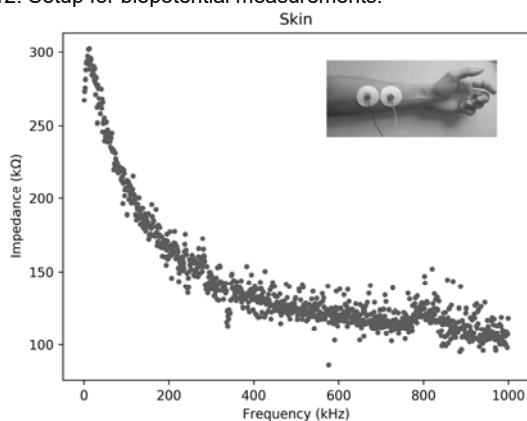
Fi.. 13. Bioimpedance measurement on hand.

For isolating our system from power line was used external power bank with step-down DC-DC converter.

Conclusions and Further Work

In this work, we present an overview of our design for potential measurement with real-time sensing signal filtering. The measurements were compared with an impedance analyzer based on board Evaluation AD5933.

The measurements were made in an isolated antistatic table, as shown in Figure 13. The impedance in low frequency is around 300 kΩ and decreases to 120 kΩ with frequency increasing.

Authors:
Inż. Oleksii Hyka, Netrix S.A, Research and Development Center, Związkowa 26, 20-148 Lublin
e-mail: oleksii.hyka@netrix.com.pl
dr inż. Andres Vejar, Netrix S.A., Research and Development Center, Związkowa 26, 20-148 Lublin, University of Economics and Innovation in Lublin, ul. Projektowa 4, 20-209 Lublin, e-mail: andres.vejar@netrix.com.pl,
dr hab. inż. Tomasz Rymarczyk, prof. Uczelni, Netrix S.A., Research and Development Center, Związkowa 26, 20-148 Lublin, University of Economics and Innovation in Lublin, ul. Projektowa 4, 20-209 Lublin, e-mail: tomasz@rymarczyk.com,

REFERENCES
[1] Rymarczyk T., Kłosowski G., Tchórzewski P., Cieplak T., Kozłowski E.: Area monitoring using the ERT method with multisensor electrodes, Przegląd Elektrotechniczny, 95(1), 153-156, 2019.
[2]. Koulountzios P., Rymarczyk T., Soleimani M., A quantitative ultrasonic travel-time tomography system for investigation of liquid compounds elaborations in industrial processes, Sensors, 19(23), 5117, 2019.
[3] Kłosowski G., Rymarczyk T., Kania K., Świć A., Cieplak T., Maintenance of industrial reactors based on deep learning driven ultrasound tomography, Eksploatacja i Niezawodnosc – Maintenance and Reliability; 22(1), 138–147, 2020.
[4] Kłosowski G., Rymarczyk T., Cieplak T., Niderla K., Skowron Ł., Quality Assessment of the Neural Algorithms on the Example of EIT-UST Hybrid Tomography, Sensors, 20(11), 3324, 2020.
[5] Rymarczyk T.: Characterization of the shape of unknown objects by inverse numerical methods, Przeglad Elektrotechniczny, 88(7B), 138-140, 2012.
[6] Rymarczyk T., Using electrical impedance tomography to monitoring flood banks 16th International Symposium on Applied Electromagnetics and Mechanics (ISEM) International journal of applied electromagnetics and mechanics, 45, 489-494, 2014.
[7] Korzeniewska,E; Szczesny, A; Lipinski, P; Drozdz, T; Kielbasa, P; Miernik, A, Prototype of a Textronic Sensor Created with a Physical Vacuum Deposition Process for Staphylococcus aureus Detection, SENSORS Volume: 21 Issue: 1 Article Number: 183, 2021.
[8] Pawlowski, S; Plewako, J; Korzeniewska, E , Influence of Structural Defects on the Resistivity and Current Flow Field in Conductive Thin Layers, ELECTRONICS Volume: 9 Issue: 12 Article Number: 2164, 2020.
[9] Woltjer, H. H., et al. "The Technique of Impedance Cardiography." European Heart Journal, vol. 18, no. 9, Sept. 1997, pp. 1396–403. DOI.org (Crossref),
[10] Bera, Tushar Kanti. "Bioelectrical Impedance Methods for Noninvasive Health Monitoring: A Review." Journal of Medical Engineering, vol. 2014, June 2014, pp. 1–28. DOI.org.
[11] Vejar, Andres, and Tomasz Rymarczyk. "Electrical Tomography Reconstruction Using Reconfigurable Waveforms in a FPGA." Sensors, vol. 21, no. 9, May 2021, p. 3272.
[12] Taji, Bahareh, et al. "Effect of Pressure on Skin-Electrode Impedance in Wearable Biomedical Measurement Devices." IEEE Transactions on Instrumentation and Measurement, vol. 67, no. 8, Aug. 2018, pp. 1900–12. DOI.org (Crossref).
[13] Rymarczyk, Tomasz, and Andres Vejar. "Multi Frequency Electrical Tomography with Reconfigurable Excitation Waveforms." 2019 Applications of Electromagnetics in Modern Engineering and Medicine (PTZE), IEEE, 2019, pp. 198–202..
[14] Rymarczyk, T., et al. "Image Reconstruction in Electrical Impedance Tomography Using a Reconfigurable FPGA System." Journal of Physics: Conference Series, vol. 1782, no. 1, Feb. 2021, p. 012033.
[15] Björklund, Sebastian, et al. "Skin Membrane Electrical Impedance Properties under the Influence of a Varying Water Gradient." Biophysical Journal, vol. 104, no. 12, June 2013, pp. 2639–50.